PHYSICAL REVIEW B VOLUME 40, NUMBER 10 1 OCTOBER 1989

Monte Carlo calculations of adsorbate structures and the role of the vibrational entropy in phase transitions at surfaces

B. N. J. Persson
Institut für Festkörperforschung der Kernforschungsanlage Jülich, D-5170 Jülich, Federal Republic of Germany
(Received 4 January 1989)

I have used the Monte Carlo method to study the ordered structures of CO on Pt(111). The calculations are based on a recently constructed potential energy surface for CO on Pt(111) and on CO-CO interaction potential deduced from the variation of the CO binding energy with coverage. The results are consistent with most known experimental facts and give additional information about adsorbate structures not directly available from experimental data. For many chemisorption systems several different substrate binding sites (e.g., atop and bridge sites) can be occupied simultaneously. The resonance frequencies of the low-frequency adsorbate vibrational modes (frustrated translations and rotations) may differ strongly between the different symmetry sites, and this introduces an important vibrational entropy term in the free energy for the adsorbate system, which at high temperature tends to favor occupation of the sites with the lowest vibrational frequencies. I show that this is a strong driving force for phase transitions in many adsorbate systems and in particular for the order-disorder transition of CO on Pt(111).

I. INTRODUCTION

The binding positions of adsorbates on surfaces is one of the central topics in surface science and enters directly in the discussion of many important processes at surfaces such as heterogeneous catalysis. The structure of ordered adsorbate systems is usually determined using low-energy electron diffraction (LEED). While this method determines the dimension of the adsorbate unit cell directly, it requires very involved calculations to determine binding positions and, if the unit cell contains more than one adsorbate, the arrangement of the adsorbates within the unit cell. In this work I show how adsorbate structures can be obtained using Monte Carlo simulations based on a potential energy surface constructed from infrared-reflection-absorption spectroscopic (IRAS) studies of adsorbate vibrations, and from information about the lateral interaction between the adsorbates as deduced from the variation in the adsorbate binding energy with coverage. For CO on Pt(111) the method reproduces most of the ordered structures observed by LEED (as a function of coverage) and provides additional information about the adsorbate system which is hard to deduce directly from experimental data. An example is the displacement of CO molecules away from the symmetry points of the substrate.

Phase transitions at surfaces have been studied both experimentally and theoretically for several years.[1] In particular, order-disorder transitions occur in a large number of adsorbate systems and provide intriguing illustrations of critical behavior in two-dimensional systems. In the case of second-order phase transitions most work has been concerned with the determination of the critical exponents and finding out in which universality class the transition falls. These properties depend on the symmetry operations of the adsorbate-substrate system and on the dimension d of the system ($d=2$ for adsorbates), but usually do not depend directly on the nature of the adsorbate-adsorbate interaction or on the nature of the potential energy surface. On the other hand, the actual value of the critical temperature T_c and the nature of the "driving force" for the phase transition depends on these latter properties. The understanding of the driving force for phase transitions is an important and interesting topic. In this work I point out the dominating role played by the vibrational entropy in many cases.

II. POTENTIAL ENERGY SURFACE AND ADSORBATE-ADSORBATE INTERACTION POTENTIAL

From IRAS[2] and electron-energy-loss spectroscopy[3] (EELS) it is known that for CO on Pt(111) only the atop and bridge sites are occupied at all adsorbate coverages and temperatures. Based on a detailed IRAS study of the temperature and coverage dependence of the internal C—O stretch vibration for this system the potential energy curve between the atop and the bridge site can be constructed (see Ref. 4) and the result is shown in Fig. 1. The CO binding energy is highest in the atop site and about 60 meV smaller in the bridge site. The activation energy for CO diffusion is determined by the height of the barrier between the atop and the bridge site and is about 0.3 eV according to Fig. 1. Note that the potential well at the atop site is very flat—the local curvature corresponds to a frustrated translation frequency for CO of about $\omega_T \approx 49$ cm^{-1}. The local curvature at the bridge site is much higher, corresponding to a frequency of $\omega_B \approx 300$ cm^{-1}. Both the activation barrier for diffusion and ω_T agree well with independent and more direct experimental measurements of these quantities.[5,6] The potential energy in the vicinity of the atop and bridge sites can be written as

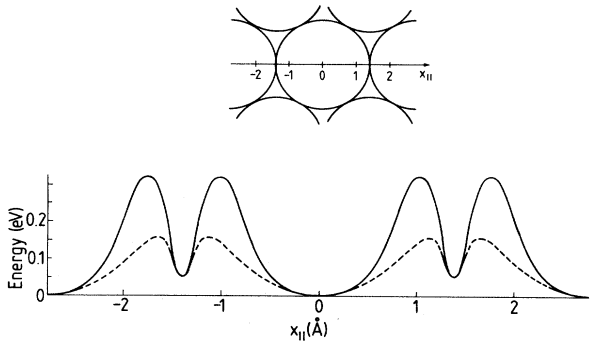

FIG. 1. Solid line: Potential energy curve between the atop and bridge sites for CO on Pt(111). Dashed line: The potential energy curve for zero anharmonicity $a=0$ from Ref. 4.

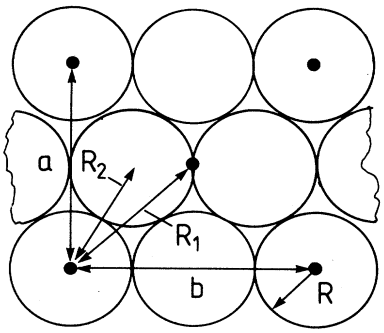

a = 4.8 Å
b = 5.5 Å
R = 1.39 Å
R_1 = 3.67 Å
(a) R_2 = 2.77 Å

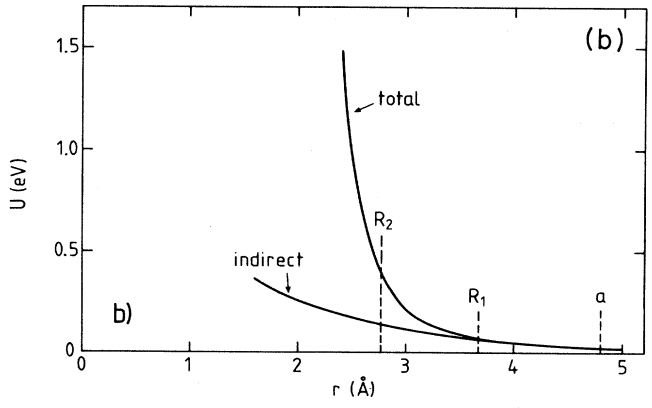

FIG. 2. (a) Binding distances in the 4×2 structure. (b) The lateral CO-CO interaction potential for CO on Pt(111).

$$U_T=\tfrac{1}{2}m\omega_T^2(1+ax^2)x^2$$

and

$$U_B=\Delta E+\tfrac{1}{2}m\omega_B^2(x-x_B)^2\ ,$$

respectively, where x_B denotes the x coordinate of the bridge site and where $\Delta E\approx 60$ meV is the difference in the CO binding energy between the atop and bridge sites. For CO on Pt(111), $a=2.61$ Å^{-2} (see Ref. 4), but I find it convenient to consider a as an external parameter and vary it continously since for other CO chemisorption systems it might be smaller or larger. The dashed line in Fig. 1 shows the potential energy curve for $a=0$.

Let us now turn to the CO-CO interaction potential. For CO on Pt(111) both the static dipole-dipole and the van der Waals interaction are very weak and can be neglected. The dominant contribution comes from the indirect interaction via the substrate[7] and from the "Pauli repulsion" which results when two CO molecules are so close that the wave functions associated with their closed shells overlap. For CO on Pt(111) the CO-CO interaction potential is purely repulsive as can be deduced from the monotonic decrease in CO binding energy as a function of increasing coverage.[8,9] The CO-CO interaction potential is therefore taken be $U(r)=Ae^{-\alpha r}+A'e^{-\alpha' r}$, where A and $A'>0$ and r is the CO-CO separation. The first term in $U(r)$ represents the Pauli repulsion. For two CO molecules with their axes aligned parallel one can deduce from thermodynamic[10] and other data[11] that $A=3.9\times 10^4$ eV and $\alpha=4.3$ Å^{-1}. We have used these values for CO on Pt(111). The second term in $U(r)$ arises from the more long-range ($\alpha'<\alpha$) interaction via the substrate. The parameters A' and α' have been determined such that (a) the CO binding energy decreases by the observed[8] 0.25 eV as the coverage increases from $\Theta=0$ to 0.5 and (b) the frequency of the frustrated translation increases from $\omega_T=49$ to 60 cm^{-1} in the same coverage range as observed in inelastic helium scattering.[6] This gives $A'=1.3$ eV and $\alpha'=0.8$ Å^{-1}. In Fig. 2(a) I show some important distances for CO on Pt(111) and in Fig. 2(b) I show the total potential $U(r)$ as well as the contribution from the indirect interaction alone.

III. MONTE CARLO SIMULATION

The Monte Carlo simulations have been done as follows. All CO molecules occupy atop or bridge sites. However, the CO molecules will in general be displaced slightly away from the symmetry points of the substrate by the unbalanced repulsive forces from the other CO molecules or simply due to the irregular thermal motion which occurs at nonzero temperatures. Figure 3 shows how the CO molecules can jump between different symmetry sites. An atop CO can jump to any of its six nearest-neighbor bridge sites, while a bridge CO can jump to one of its two nearby atop sites. In these jumps we allow for small random displacements away from the symmetry points. Furthermore, after each jump we allow the CO molecules to readjust and thermalize in the wells. Any tentative change in the adsorbate positions is accepted or rejected according to the standard Monte Carlo

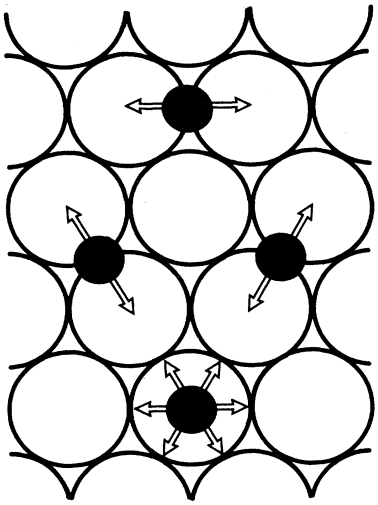

FIG. 3. Allowed jumps between different symmetry sites.

prescription[12] so that after long enough time the system will reach thermal equilibrium independent of the initial conditions. All calculations have been made using periodic boundary conditions with the basic unit containing $M \times M$ Pt atoms, where M has been varied (typically $M=6$, 8, or 10). The CO molecules are placed initially in atop positions on one side of the basic unit as in Fig. 4, and the number N of CO molecules in the basic unit determines the CO coverage via $\Theta=N/M^2$. Figure 4 shows, as an example, the result of a Monte Carlo calculation with 32 CO molecules on an 8×8 unit, i.e., at $\Theta=0.5$ and at the temperature $T=250$ K. After 20 MC steps per particle only one CO molecule has changed sites. After 1000 MC steps per particle about half of the CO molecules have jumped (diffused) away from their original sites and after 100 000 MC steps per particle an almost perfect (4×2) structure is obtained, as is indeed observed experimentally. In addition to the vibrational excitations which give rise to small random displacements of the CO molecules away from the substrate symmetry points, one nonvibrational excitation occurs (denoted by T^* in the figure). Here a bridge CO has jumped over the barrier between a bridge and an atop site, but because of the repulsive forces from the other nearby atop CO molecules, the CO molecule remains displaced by about 0.4 Å towards the original bridge site. This is the lowest-energy nonvibrational excitation in the system and is very important for the room-temperature properties of the adsorbate system (see Ref. 4 and below).

The Monte Carlo simulations presented in this paper are based on classical statistical mechanics, i.e., all quantum effects are neglected. This is certainly a good approximation for the vibrational motion of atop bonded CO since the parallel frustrated translation is in this case highly excited for all relevant temperatures. However, the frequency of the frustrated translation of bridge bonded CO is quite high, and this mode is only weakly excited even at room temperature. To estimate the accuracy of using classical statistical mechanics in the present case let us consider the change in the vibrational free energy as an on top CO molecule is transferred to a bridge site (this is an important driving force for phase transitions, see below). Quantum mechanically this quantity is given by

$$2k_BT\ln\left[\frac{1-e^{-\beta\omega_T}}{1-e^{-\beta\omega_B}}\right],$$

while classically it is

$$2k_BT\ln\left[\frac{\omega_T}{\omega_B}\right].$$

At room temperature these equations give -63 and -89 meV, respectively. Note, however, that for ordered ad-

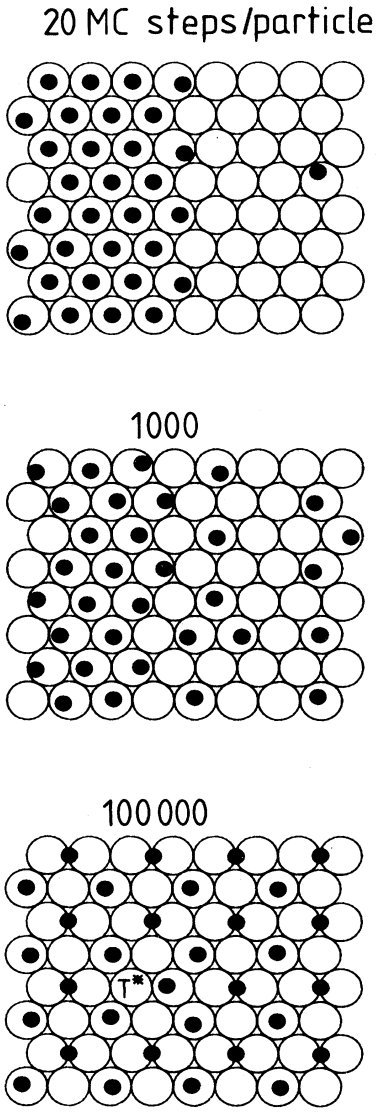

FIG. 4. The results of a Monte Carlo calculation at $T=250$ K.

sorbate structures at low temperature, there is no difference between the quantum and the classical solutions since the vibrational free energy vanishes at $T \to 0$. The same is true for the large adsorbate displacements away from the substrate symmetry points which occurs in disordered or compressed adsorbate structures as well as for the displacements involved in nonvibrational excitations such as the T^* excitation discussed above.

IV. ORDERED STRUCTURES AT $T = 50$ K

Figure 5 shows the variation in the relative CO bridge coverage N_B/N as a function of the coverage Θ. The circles are the Monte Carlo results at 50 K obtained by cooling the system very slowly (typically in 300 000 MC steps per particle) from $T = 500$ K. At low CO coverage only atop sites are occupied which is easy to understand since this site has the largest binding energy and the temperature is not high enough to thermally populate the bridge sites. As the coverage increases above $\Theta = \frac{1}{3}$, the bridge sites start to become occupied. This results from the repulsive CO-CO interaction which tends to spread out the CO molecules as uniformly as possible on the surface. At $\Theta = \frac{1}{2}$ half of the CO molecules occupy the bridge sites. As Θ increases beyond $\frac{1}{2}$, the relative bridge coverage decreases so that finally at $\Theta = 1$ all the atop sites are occupied with zero-bridge-site occupation. The arrows in Fig. 5 indicate those coverages where ordered CO structures are obtained. These coverages agree exactly with those where ordered patterns are observed in LEED (except for $\Theta = 1$ which cannot be reached experimentally before the CO molecules starts to desorb). In Fig. 6 I show the resulting ordered patterns at $\Theta = \frac{1}{3}$, $\frac{1}{2}$, $\frac{2}{3}$, and 0.6. The triangular structure at $\Theta = \frac{1}{3}$ is easy to understand physically—it follows directly from the fact that the atop sites have the largest binding energy and that the triangular adsorbate structure minimizes the total CO-CO interaction energy. However, the structures at $\Theta = \frac{1}{2}$, $\frac{2}{3}$, and 0.6 are far from trivial. They result from the competition between the larger binding energy in the atop sites and the repulsive CO-CO interaction potential which favors a uniform adsorbate distribution and hence forces some CO molecules to occupy the bridge sites. While most workers agree that the structures I obtain at $\Theta = \frac{1}{3}$ and $\frac{1}{2}$ are correct[13] there exists some controversy concerning the structure of the so-called "compressed" adsorbate structures at $\Theta = 0.6$ and $\frac{2}{3}$. Based on a LEED study, Tracy and Palmberg[14] have suggested that for $\Theta > 0.5$ uniformly compressed structures occur where the adsorbates are out of registry with the substrate atoms. However, the structure at $\Theta = \frac{2}{3}$ shown in Fig. 6 agrees with that proposed by Avery[15] and by Biberion and Van Hove[16] based on detailed LEED and EELS studies. At

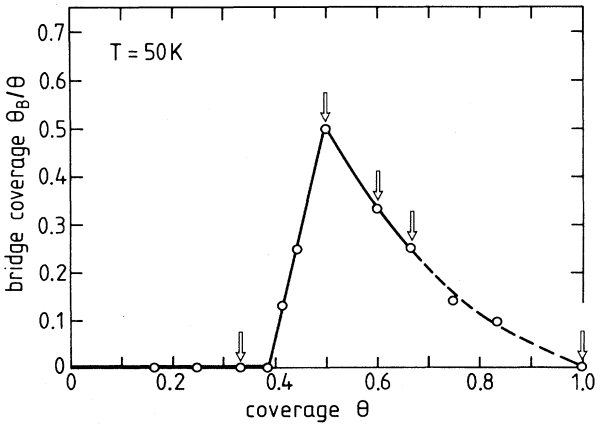

FIG. 5. The relative bridge coverage as a function of the coverage. The arrows indicate the coverages where ordered structures are observed. The circles are the Monte Carlo result obtained by slowly cooling down from $T = 500$ to 50 K in about 300 000 MC steps per particle.

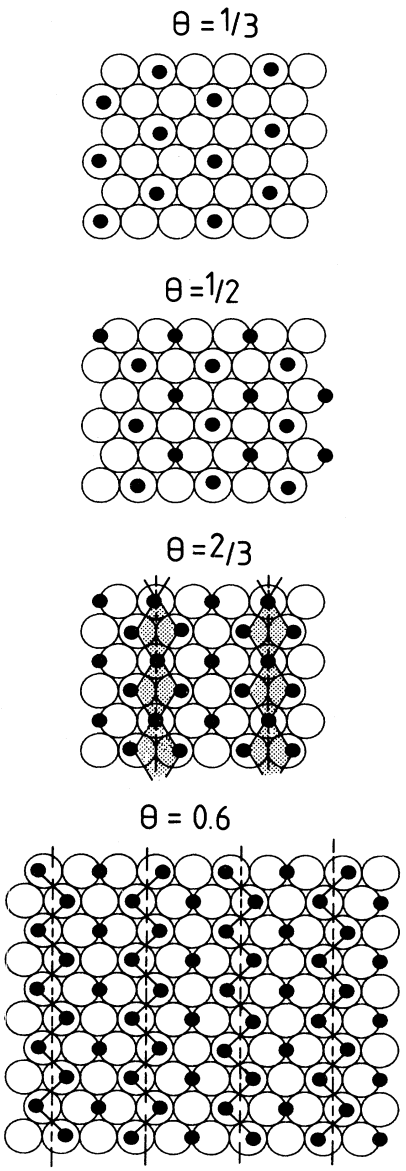

FIG. 6. The ordered structures at four different coverages at $T = 50$ K.

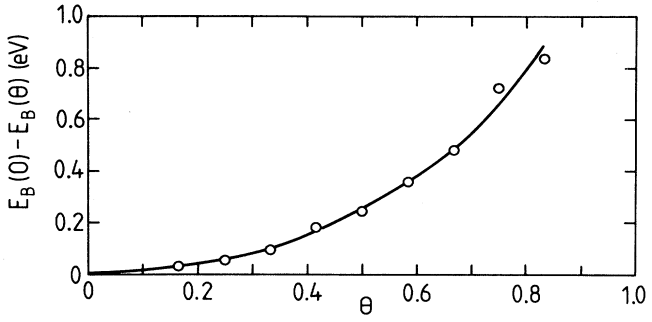

FIG. 7. The change in the CO binding energy as a function of coverage at $T=50$ K.

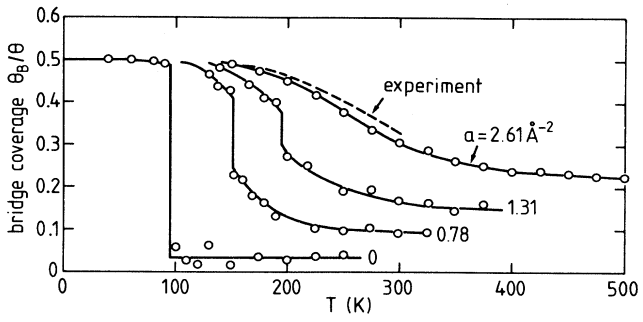

FIG. 8. The relative bridge coverage as a function of temperature and for 4 different anharmonicity parameters. The dashed curve is deduced from IRAS-data, see Ref. 4.

$\Theta=0.6$, Avery presented a different structure from the one shown in Fig. 6 while Biberion and Van Hove arrived at the structure shown in Fig. 6. The compressed structures in Fig. 6 consist of vertical strips of $c(4\times2)$ structure separated by high-density antiphase boundaries. At these antiphase boundaries the atop CO molecules are shifted away from their symmetry sites because of the unbalanced repulsive CO-CO interactions. These displacements are ≈0.4 Å and imply a tilted C—O bond axis (about 10°) in order for the C—O bond axis to point to the center of the neighboring metal atom. This results in a dipole active frustrated rotation, which explains why this mode is seen in EELS (dipole scattering) from compressed adsorbate structures.[17] To the discussion above we must add the following reservation. In the simulations of the ordered structures (see Fig. 6) I have used relative small basic units ($M=6$ and 10). If other or alternative ordered structures would exist which would not fit within the basic unit (e.g., incompatible with the periodic boundary conditions) then these structures could not be obtained in the presented simulation.

In Fig. 7 we show how the energy per CO molecule (i.e., the total energy divided by the number of CO molecules) varies with the CO coverage. The drop in the energy between $\Theta=0$ and 0.5 (≈0.25 eV) agrees with that measured by Ertl *et al.*[8] However, Ertl *et al.* observed very sharp, almost steplike, changes in the binding energy at $\Theta=\frac{1}{2}$ and $\frac{2}{3}$, but in a more recent study Seebauer *et al.*[9] find a smoothly varying CO binding energy in accordance with the present results.

V. PHASE DIAGRAM AT $\Theta=0.5$

In Fig. 8 I show the variation in the relative bridge occupation as a function of temperature at the coverage $\Theta=0.5$. At low temperature the (4×2) structure shown in Fig. 4 prevails where half the CO molecules occupy the bridge sites and half the atop sites so that $\Theta_B/\Theta=0.5$. The circles are the result of the Monte Carlo calculations for four different anharmonicity values, namely $a=0$, 0.78, 1.31, and 2.61 Å^{-2}. The dashed line is deduced from IRAS data, see Ref. 4. For $a=0$ there is a steplike change in the bridge occupation at $T\approx90$ K. Since the distribution of CO molecules changes discontinuously at this temperature this must be a first-order phase transition. Furthermore, it is a transition from the ordered (4×2) structure to another ordered structure (8×4) as shown in Fig. 9. The driving force for this transition is due entirely to the change in the vibrational entropy, as can be proved as follows: The transition temperature T_c is the temperature where the change in free energy $\Delta F=F(8\times4)-F(4\times2)=0$. Let $\mathcal{E}$ denote the increase in the internal energy per particle when going from the (4×2) to the (8×4) structure. It is easy to calculate $\mathcal{E}=11.6$ meV. If N denotes the total number of CO molecules we get

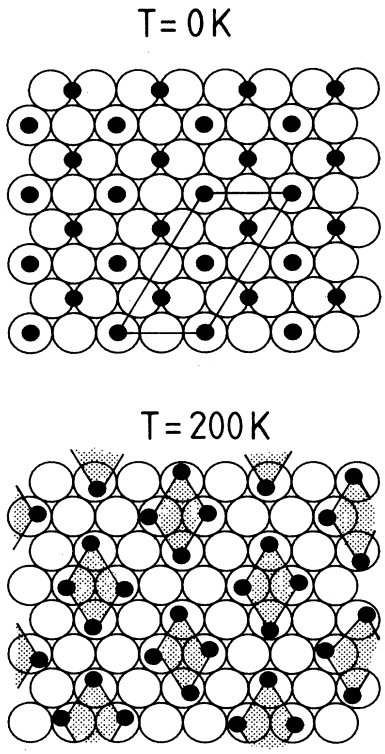

FIG. 9. The ordered structures 4×2 and 8×4 observed at two different temperatures and for the anharmonicity parameter $a=0$.

$$\Delta F = N\mathcal{E} - N\left[2k_BT\ln\frac{k_BT}{\omega_{T'}} - k_BT\ln\frac{k_BT}{\omega_B} - k_BT\ln\frac{k_BT}{\omega_T}\right]$$
$$= N\left[\mathcal{E} - k_BT\ln\frac{\omega_B\omega_T}{\omega_{T'}\omega_{T'}}\right]$$

and the condition $\Delta F = 0$ gives

$$k_BT_c = \frac{\mathcal{E}}{\ln(\omega_B\omega_T/\omega_{T'}\omega_{T'})} . \quad (1)$$

The terms involving the logarithmic functions are the contribution from the vibrational motion to the free energy. Numerical calculations show that in the absence of anharmonicity (i.e., $a=0$), the effective resonance frequency for the frustrated translation $\omega_{T'}$ of the atop CO molecules in the displaced state occurring in the (8×4) structure is practically identical to that in the (4×2) structure, i.e., $\omega_{T'}\approx 65$ cm^{-1}, while $\omega_{T'}\approx 60$ cm^{-1} [the frequency $\omega_{T'}$ was obtained by deducing $\langle \mathbf{x}^2\rangle - \langle \mathbf{x}\rangle^2$ ($\mathbf{x}$ is the displacement vector away from the atop symmetry site) from the MC calculation and identifying this with that for a two-dimensional isotropic oscillator, i.e., $2k_BT/m\omega_{T'}^2$]. Using the equation above with $\omega_B = 300$ cm^{-1} gives $\Delta F = 0$ when $T_c = 96$ K in good agreement with the result of the Monte Carlo simulation. This proves that the driving force for the phase transition is due entirely to the change in vibrational entropy.

As the anharmonicity parameter a increases, the change in the internal energy $N\mathcal{E}$ and the effective resonance frequency $\omega_{T'}$ increase. According to (1) both effects tend to increase the transition temperature. This is consistent with Fig. 8 where $T_c = 151$ and 195 K for $a = 0.78$ and 1.31 Å^{-2}, respectively. However, for $a > 0$, the transition temperature T_c is no longer accurately given by (1) (see dash-dotted line in Fig. 10) because both the 4×2 and the 8×4 structures are disordered at T_c and this disorder gives an entropy contribution to the free energy and affects also the internal energy. For $a > 2.26$ Å^{-2} no steplike change in the bridge occupation occurs which indicates a second-order phase transition where the probability distribution for the adsorbate positions changes continuously with temperature, or else a weakly first-order transition which can be almost indistinguishable from a second-order phase transition.[18] Furthermore, for example, $a = 2.61$ Å^{-2} which corresponds to the actual value of the anharmonicity parameter for the CO/Pt(111) system, no ordered phase exists above T_c, i.e., the transition is now an order-disorder transition. In Fig. 10 I show the resulting phase diagram where the solid and dashed lines denote first- and second-order phase-transition lines, respectively. Numerical studies indicate that the boundary line between the 8×4 and the disordered phase is a second-order phase-transition line, but it is very difficult to prove numerically whether this line joins exactly at a tricritical point (the point where the first-order phase-transition line switches into a second-order line) as indicated in the figure. Since for $a > 2.26$ Å^{-2} a second-order phase transition occurs, the critical temperature T_c cannot be obtained from the temperature dependence of the bridge coverage as this quantity now varies continuously with coverage. However, the specific heat has a singularity at $T = T_c$ which for a finite system (in this case an 8×8 unit with periodic boundary conditions) becomes a broad peak as shown in Fig. 11. The "background" value $C/k_B = 1$ indicated by the dashed line in this figure is the contribution to the heat capacity from the small-amplitude vibrational motion of the CO molecules around their local equilibrium positions. The

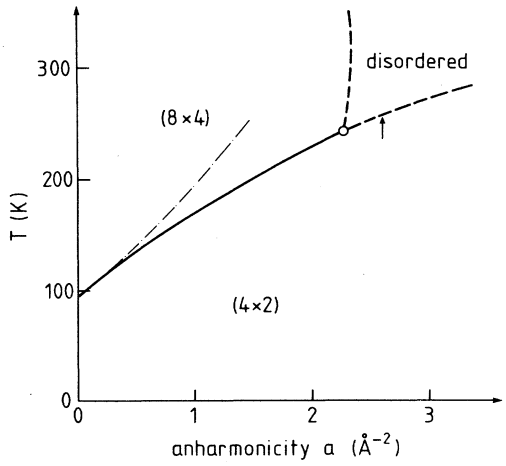

FIG. 10. Phase diagram. The solid curve denotes a first-order phase-transition line, while the dashed lines are second-order phase-transition lines. The arrow indicates the anharmonicity parameter for CO on Pt(111). The dash-dotted line is calculated from Eq. (1).

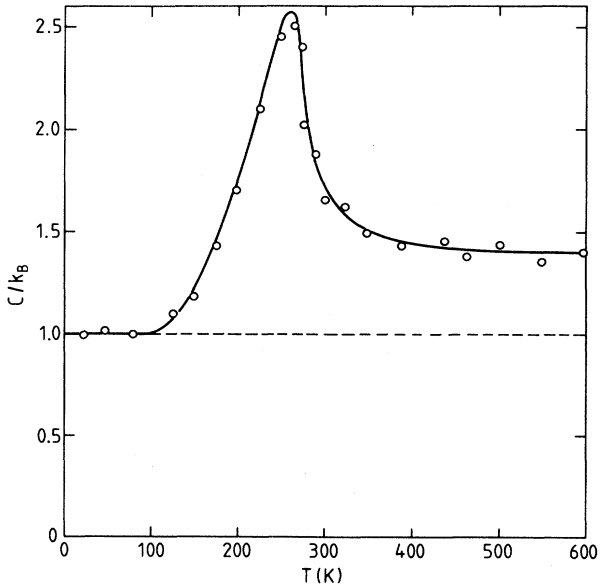

FIG. 11. The heat capacity for $a = 2.61$ corresponding to CO on Pt(111). The dashed lines indicate the contribution to C from the vibrational motion.

additional contribution to C which peaks at $T \approx 260$ K is derived from configurational changes in the particle distribution, i.e., from CO molecules performing jumps between different symmetry sites. From Fig. 11 we obtain $T_c \approx 260$ K which agrees well with the experimental transition temperature $T_c(\text{expt}) \approx 275$ K as deduced from the temperature dependence of the LEED spot intensity of a LEED spot associated with the 4×2 structure.[4] In agreement with the theoretical results presented above, the LEED data also shows that the transition is of the order-disorder type since no new diffraction spots occur on the LEED picture for $T > T_c$. The dominant driving force for the order-disorder transition is again the change in vibrational entropy as a bridge CO is transferred to an atop site as can be proved as follows: Note first that the 4×2 structure is degenerate. That is, there are several symmetry operations which take this structure into itself. On such symmetry operation consists of displacing all the CO molecules by a radius R to the right (or to the left) along the x direction in Fig. 12. This moves all atop bonded CO molecules to bridge sites and vice versa. At the interface between two such (4×2) "grains" an interface free energy f will be stored. The interface is stable for $T < T_c$, but for $T > T_c$ a unique disordered phase exists, i.e., $f \to 0$ as $T \to T_c$ if the phase transition is of the second-order type. More precisely, in the present case where several different interfaces can be formed, the free energy associated with all these interfaces must vanish at $T = T_c$. Consider the interface shown in Fig. 12 which for $T < T_c$ probably has the lowest free energy of all possible interfaces. Let ε denote the energy per unit length it cost to create this interface. This quantity can be calculated by subtracting the total energy of a finite unit cell having an interface with the total energy of a similar unit without an interface and dividing the result with the length of the interface. In the present case this gives $\varepsilon = 44$ meV (the unit of length is taken to be $4R$, i.e., the side of the 4×2 unit in the x direction). When an interface of the type shown in Fig. 12 is formed, the number of bridge-bonded CO molecules decreases, and the number of atop CO molecules increases. Accounting for this contribution to the vibrational entropy gives the following interface free energy per unit length:

$$f = \varepsilon - k_B T \ln \frac{\omega_B \omega_T^3}{\omega_{T''}^4} - k_B T S_{\text{kink}} ,$$

where S_{kink} is the entropy (in units of k_B) contribution associated with the fact that the "grain" boundary in general is not flat as shown in Fig. 12 but rough, i.e., it has "kinks" and more complex structure in the vertical direction,[19] and $\omega_{T''}$ is the resonance frequency of the displaced atop CO molecules at the interface. The condition $f = 0$ gives

$$k_B T_c = \frac{\varepsilon}{\ln(\omega_B \omega_T^3 / \omega_{T''}^4) + S_{\text{kink}}} .$$

Monte Carlo simulations show that $\omega_{T''} \approx 70$ cm^{-1} and hence $\ln(\omega_B \omega_T^3 / \omega_{T''}^4) \approx 1$. Since $k_B T_c \approx 22$ meV ($T_c = 260$ K) we must have $S_{\text{kink}} \approx 1$ at $T = T_c$ (note that S_{kink} depends on temperature). Hence we conclude that at least 50% of the interface entropy is derived from the change in the vibrational entropy. Actually, the contribution may be even larger because it is very likely that the kinks are stabilized by vibrational entropy.

In a second-order phase transition for temperatures close to the critical temperature large fluctuations occur. Hence, for example, an order-disorder transitions, for $T > T_c$ (but T close to T_c) the adsorbate layer is not completely disordered on all length scales. It is certainly true that for $T > T_c$ no infinite long-ranged correlation occurs, but there will be finite regions where the adsorbates are locally ordered in the structure which prevails for $T < T_c$. These regions of short-range correlation fluctuate in time and become spatially smaller and more short lived as T increases away from T_c. Figure 13 illustrates schematically how the CO-Pt(111) system may look at a particular time for $T \approx 300$ K and $a = 2.61$ Å^{-2}. Since we are rela-

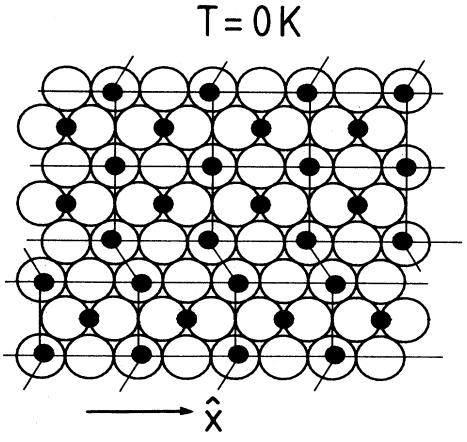

FIG. 12. Interfaces between two 4×2 grains. Note that two interfaces exist because of the periodic boundary conditions.

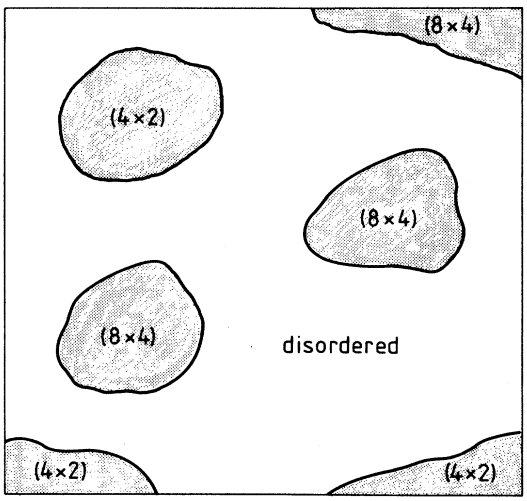

FIG. 13. A schematic picture which illustrates how the CO/Pt(111) overlayer system might look at a particular time in the disordered phase but close to the 4×2 and 8×4 order-disorder lines.

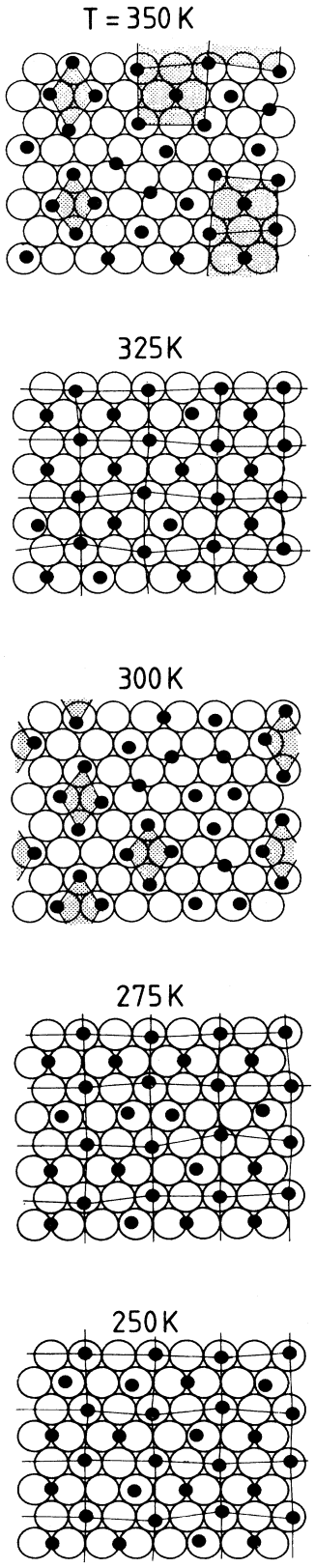

FIG. 14. The result of a series of Monte Carlo simulations for increasing temperature and with the anharmonicity parameter $a = 2.61$ Å^{-2}

tively close to the 8×4 and 4×2 order-disorder boundaries, we expect spatially and temporally to have islands of ordered 8×4 and 4×2 structures surrounded by a disordered "phase." This basic picture is nicely illustrated by the results of our Monte Carlo simulation. Figure 14 shows the result of a series of Monte Carlo calculations for decreasing temperatures. Note the large fluctuations; at $T=300$ K the MC picture is disordered with some tendency for the 8×4 structure to form, while at 325 K an ordered 4×2 structure is obtained. Of course, if we had a truly infinite system and not just a small basic unit with periodic boundary conditions, then only finite regions of 8×4 and 4×2 structures would result as in Fig. 13. Note also that at $T=325$ K a little later in time (i.e., after a few more Monte Carlo steps) the ordered structures have disappeared and are replaced by disorder, i.e., the system fluctuates in time. Large fluctuations between the disorder and the 8×4 structure occur in the whole high-temperature region studied ($300\text{ K} < T < 600$ K) because the phase-transition line between the 8×4 and the disordered structures are close to and almost parallel with the line $a=2.61$ Å^{-2} in the (a,T) phase diagram. This also explains why the heat capacity seemingly saturates at a value $C/k_B > 1$ for $T > 300$ K instead of decreasing back towards $C/k_B = 1$ as expected if with increasing temperature one would move away from all phase-transition lines.

Based on the Monte Carlo simulations presented above I have argued that the dashed lines in Fig. 10 are second-order-phase transition lines since the bridge coverage seems to vary continuously at the transition temperature. However, without very extensive MC simulations it is not possible to definitively prove if this is true.

The results presented above should be very general since CO chemisorption on all the transition metals occurs in a similar way with relative small variations in the potential energy surface. In particular, in all cases one would expect the frequency for the frustrated translation of atop bonded CO to be very low giving rise to a strong tendency for this site to be occupied at high temperatures. For example, for CO on Ni(100) using inelastic helium scattering the Toennies group[20] has determined $\omega_T \approx 28$ cm^{-1}. I also expect that the results presented above will be valid for many other chemisorption systems involving small molecules, e.g., NO.

VI. SUMMARY AND CONCLUSION

In this work I have presented a Monte Carlo simulation study of the ground state and thermal properties of the CO/Pt(111) chemisorption system. The calculations are based on a potential energy surface constructed from a detailed IRAS study[4] of the C—O stretch vibration, and on the lateral CO-CO interaction potential deduced from thermodynamic data for gas phase and adsorbed CO. All the results of the Monte Carlo calculation are in excellent agreement with the experimental data of Schweizer *et al.*[4]

Many Monte Carlo calculations of adsorbate phase diagrams have been presented in the literature. The calculations are usually based on the lattice-gas model, where

the ad atoms or molecules occupy specific high-symmetry sites without allowing for any vibrational motion or displacement away from the symmetry sites (however, see Ref. 21). In the present case such a model would fail qualitatively since the major driving force for phase transitions comes from the variation of the vibrational entropy between different symmetry sites. For example, a lattice-gas model would in the present case give an order-disorder transition at approximately twice as high T_c as obtained above.

ACKNOWLEDGMENTS

I would like to thank A. M. Bradshaw, J. Harris, D. Hoge, R. O. Jones, P. Rujan, W. Selke, E. Schweizer, E. Tosatti, J. P. Toennies, M. Tushaus, and J. Villain for many useful discussions.

[1]See *Proceedings of the Symposium on Statistical Mechanics of Adsorption, Trieste, Italy,* 1982, edited by M. W. Cole, F. Toigo, and E. Tosatti [Surf. Sci. **125**, 1 (1983)]; M. Schick, Prog. Surf. Sci. **11**, 245 (1981); E. Bauer, in *Structure and Dynamics of Surfaces II,* edited by W. Schommers and P. von Blanckenhagen (Springer, Berlin, 1987), p. 115; L. D. Roelofs, in *Chemistry and Physics of Solid Surfaces IV,* edited by R. Vanselow and R. Howe (Springer, Berlin, 1988); T. L. Einstein, *Chemistry and Physics of Solid Surfaces VII,* edited by R. Vanselow and R. How (Springer, Berlin, 1988), p. 307.

[2]R. G. Tobin and P. L. Richards, Surf. Sci. **179**, 387 (1987).

[3]H. Steininger, S. Lehwald, and H. Ibach, Surf. Sci. **123**, 264 (1982).

[4]E. Schweizer, B. N. J. Persson, M. Tüshaus, D. Hoge, and A. M. Bradshaw, Surface Sci. **213**, 49 (1989).

[5]B. Poelsema, L. K. Verheij, and G. Comsa, Phys. Rev. Lett. **49**, 1731 (1982).

[6]A. M. Lahee, J. P. Toennies, and Ch. Wöll, Surf. Sci. **177**, 371 (1986).

[7]T. L. Einstein and J. R. Schrieffer, Phys. Rev. B **7**, 3629 (1973); T. B. Grimley, Proc. Phys. Soc. **90**, 751 (1967); T. L. Einstein, Surf. Sci. **75**, L161 (1978).

[8]G. Ertl, M. Neumann, and K. M. Streit, Surf. Sci. **64**, 393 (1977).

[9]E. G. Seebauer, A. C. F. Kong, and L. D. Schmidt, Surf. Sci. **176**, 134 (1986).

[10]E. A. Mason and W. E. Rice, J. Chem. Phys. **22**, 843 (1954).

[11]T. Kihara and H. Koide, Adv. Chem. Phys. **33**, 52 (1975).

[12]See, e.g., *Monte Carlo Methods in Statistical Physics,* edited by K. Binder (Springer, New York, 1979).

[13]Actually, the LEED pattern at the coverage $\Theta=\frac{1}{3}$ is rather diffuse, i.e., no perfect ordered structure exists at this coverage. At low temperature two sharp LEED patterns are observed at slightly lower coverages, see Ref. 3. These structures have very large unit cells, and I have made no attempt to find out if these structures can be obtained based on the present model. For a discussion of these low-coverage structures, see M. Tushaus, E. Schweizer, P. Hollins, and A. M. Bradshaw, J. Electron. Spectrosc. **44**, 305 (1987).

[14]J. C. Tracy and P. W. Palmberg, J. Chem. Phys. **51**, 4852 (1969).

[15]N. Avery, J. Chem. Phys. **74**, 4202 (1981).

[16]J. P. Biberion and M. A. Van Hove, Surf. Sci. **118**, 361 (1982).

[17]A. M. Baro and H. Ibach, J. Chem. Phys. **71**, 4812 (1979); P. Uvdal, P.-A. Karlsson, C. Nyberg, S. Andersson, and N. V. Richardson, Surf. Sci. **202**, 167 (1988).

[18]See, e.g., K. Binder, Rep. Prog. Phys. **50**, 783 (1987); J. Stat. Phys. **24**, 69 (1981); N. C. Bartel, T. L. Einstein, and L. D. Roelofs, Phys. Rev. B **35**, 6786 (1987). The Landau theory of second-order phase transitions indicates that all phase-transition lines are of the first-order type (E. Tosatti, private discussion).

[19]E. Muller-Hartmann and J. Zittartz, Z. Phys. B **27**, 261 (1977); J. Villain and I. Vilfan, Surf. Sci. **199**, 165 (1988).

[20]R. Berndt, J. P. Toennies, and Ch. Woll, J. Electron. Spectrosc. Phenom. **44**, 183 (1987).

[21]D. A. Huse, Phys. Rev. B **29**, 5031 (1984); S. L. Tang, M. B. Lee, Q. Y. Yang, J. D. Beckerle, and S. T. Ceyer, J. Chem. Phys. **84**, 1876 (1986); M. S. Daw and S. M. Foiles, Phys. Rev. Lett. **59**, 2756 (1987).